An Experimental Investigation of Temperature Changes During Electroporation

Paulo A. Garcia, Robert E. Neal II, Michael B. Sano, John L. Robertson, Rafael V. Davalos[*]

[1]School of Biomedical Engineering and Sciences, Virginia Tech – Wake Forest University, 330 ICTAS Bldg., Stanger Street, Blacksburg, VA 24061 USA. davalos@vt.edu

Abstract

Electroporation uses short, pulsed electric fields to induce a cellular transmembrane potential that results in increased cellular permeability. When performed irreversibly, it results in cell death while leaving the extracellular matrix and other sensitive structures intact. These electric fields result in thermal effects to the affected tissues due to resistive heating. We measure this heating extent in an *ex-vivo* canine brain by recording temperature changes in real time. Temperatures were measured at three locations near the electrodes. Thermal damage was evaluated using the Arrhenius equation. This study experimentally shows that typical electroporation protocols result in negligible thermal damage.

1. Introduction

Non-thermal irreversible electroporation (IRE) is a new minimally invasive technique to focally ablate volumes of undesired tissue [1]. The procedure involves placing electrodes in or around the area to be ablated and delivering a series of low energy (high amplitude, short duration) electric pulses. The pulses generate an electric field which induces a transmembrane potential (TMP) on cells in the exposed tissue. When the TMP and energy from the procedure reaches above a certain threshold, the membrane is unable to recover and cell death is induced [2].

IRE has proven to be an exciting new effective anti-cancer treatment in the prostate, liver, kidney and lungs [3]. Due to immediate changes in the affected tissue's permeability, the treated regions may be monitored in real-time using conventional imaging techniques including ultrasound [4], MRI [5, 6], or electrical impedance tomography [7, 8]. Treatment may be administered through small needle electrodes, making the treatments minimally invasive [9, 10]. IRE therapies have been shown to leave the major blood vessels, extracellular matrix, and other sensitive tissue architecture intact, allowing for rapid lesion resolution and minimal scarring of the treated volume [10-12].

The main difference between IRE and other focal ablation techniques such as radiofrequency (RF) ablation, high-intensity focused ultrasound (HIFU), laser interstitial thermal therapy (LITT) or cryoablation is that the mechanism of cell death does not depend on thermal energy [1, 13]. In thermal techniques, targeted regions are exposed to extreme temperatures in order to kill the tissue by coagulation necrosis, cell death, or vascular stasis followed by ischemia [14]. Because IRE technology uses lower energy than the previously mentioned procedures, it has been postulated that cell death is solely caused by altering the transmembrane potential of the cells exposed to electric fields generating loss of cell homeostasis [2].

Because electroporation based therapies require high-voltage pulses to be administered to the tissue, thermistors and thermocouples may become damaged during treatment. Therefore, these previous investigations have relied on numerical modeling, typically using a modified Pennes Bioheat equation with an added Joule heating term to predict the thermal effects resulting from IRE therapies. There have been several theoretical attempts in the literature to investigate the thermal response of tissues to IRE treatments [1, 13, 15-17].

We hypothesize that we can experimentally validate the non-thermal effects of IRE therapies. This study validates the assertion that IRE therapies cause minimal thermal damage by experimentally measuring the changes in temperature from a typical therapeutic protocol administered on an *ex-vivo* canine brain.

2. Methods

Temperature Experiments

The experimental study was performed on an *ex-vivo* canine brain 4 hours post-mortem. By this time, the brain had reached equilibrium with the room temperature (21°C). IRE pulses were delivered using the NanoKnife® (Angiodynamics, Queensbury, NY USA) pulse generator system, and two single-pole needle electrodes. The electrodes were 1 mm in diameter with a sharpened tip and exposed length of 1 cm, separated by 1 cm. Two different IRE protocols were used, one in each of the cerebral hemispheres. The tips of the electrodes were placed 2.0 cm below the brain surface within the white matter. These anatomical locations were identical to previous *in-vivo* studies that

978-1-4244-6051-9/11/$26.00 ©2011 IEEE

investigated the safety of intracranial IRE procedures [6]. Pulses were delivered in trains of 10 at 1.5 Hz for 1000 and 2000 V applied to the electrodes for 90 total pulses, each l00 µs long.

Temperatures were measured in the brain during the experiment using the Luxtron® m3300 Biomedical Lab Kit Fluoroptic® Thermometer (LumaSense™ Technologies, Santa Clara, CA USA). Three STB medical fiber optic probes (LumaSense™ Technologies, Santa Clara, CA USA) were placed at specific locations in relation to one IRE electrode (±2.5mm and +5mm) using a custom-made probe placement device (**Error! Reference source not found.**). The data acquisition was performed with TrueTemp™ software (Version 2.0, Luxtron® Corporation, Santa Clara, CA USA) in which each probe was set to a recording frequency of 2 Hz.

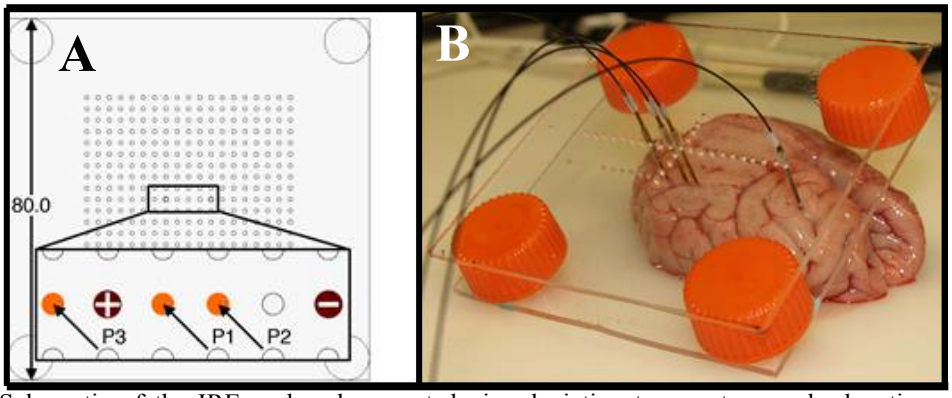

Figure 1. (A) Schematic of the IRE probe placement device depicting temperature probe locations (Dimensions in mm). Experimental placement of the probes (orange) relative to the electrodes (maroon). (B) Experimental setup used with the electrodes and thermal probes inserted into the brain.

Thermal Damage Evaluation

Thermal damage occurs when tissues are exposed to temperatures higher than their physiological temperature for extended periods of time. This damage can represent a variety of damage processes including cell death, microvascular blood flow stasis and/or protein coagulation [14]. The damage can be quantified using an Arrhenius type analysis which assumes that the damage follows first order reaction kinetics given by:

$$\Omega(t) = \int_0^\tau \zeta \cdot e^{-E_a/(R \cdot T(t))}\, dt \tag{1}$$

Where ζ is the frequency factor, E_a the activation energy, R the universal gas constant, $T(t)$ is the temperature distribution and τ is the heating time [15]. The thermal damage index (Ω) is exponentially dependant on the temperature and linearly dependant on heating time. It is convenient to express the thermal damage index as a damage probability given by

$$Damage\ (\%) = 100 \cdot \left(1 - e^{-\Omega(t)}\right) \tag{2}$$

Eqn. 2 calculates a damage probability of 0% for an index Ω = 0 and a damage probability of 99% for an index of Ω = 4.60. The damage probability was calculated for the experimental data with the parameters from Table 1.

Table 1: Activation energy (E_a) and frequency factor (ζ) for thermal damage processes [14].

DAMAGE PROCESS	E_a [J mol^{-1}]	ζ [s^{-1}]	REFERENCE
Microvascular Blood Flow Stasis	**6.670 x 10^{5}**	**1.98 x 10^{106}**	**[18]**
Cell Death	**5.064 x 10^{5}**	**2.984 x 10^{80}**	**[19]**
Protein Coagulation	**2.577 x 10^{5}**	**7.39 x 10^{37}**	**[20]**

The temperature data from the experimental model was imported for analysis into Wolfram Mathematica 6.0 for students (Champaign, IL USA). The measured temperatures were scaled by 16°C for thermal damage calculations in order to match the typical *in-vivo* canine physiological temperature of 37 °C. The highly oscillatory data was smoothed with the "MovingAverage" command in which each data point reported is the average of the neighboring 50 points. The smoothed data set was then converted into a mathematical function of time with the "Interpolation" command. The functions were evaluated numerically using Eqn. 2 to get the thermal damage probabilities.

3. Results

Figure 2 where temperature was recorded for 30 seconds before to 360 seconds after IRE pulse administration in order to allow for heat dissipation. From these, an onset and exponential temperature increase of the brain tissue is seen during administration of the electric pulses, followed by a logarithmic decay after pulsing was completed. The maximum temperatures occurred at the end of the final pulse, when all the energy was deposited in the tissue. For the 1000 V/cm case, mild temperature changes were observed with a 2 °C maximum difference. The 2000 V/cm treatment showed a maximum difference of 11.2 °C. The minimum and maximum temperatures observed by all probes during the experiment may be seen in **Table 2**.

Table 2: Temperature extremes detected from the ex-vivo IRE protocol.

PROTOCOL	TEMP. P1 [°C]	TEMP. P2 [°C]	TEMP. P3 [°C]
1000 V/cm - Min	21.3	21.3	20.4
1000 V/cm - Max	23.3	23.1	21.6
Difference	2.0	1.8	1.2
2000 V/cm - Min	21.1	20.9	20.4
2000 V/cm - Max	32.3	28.0	25.3
Difference	11.2	7.1	4.9

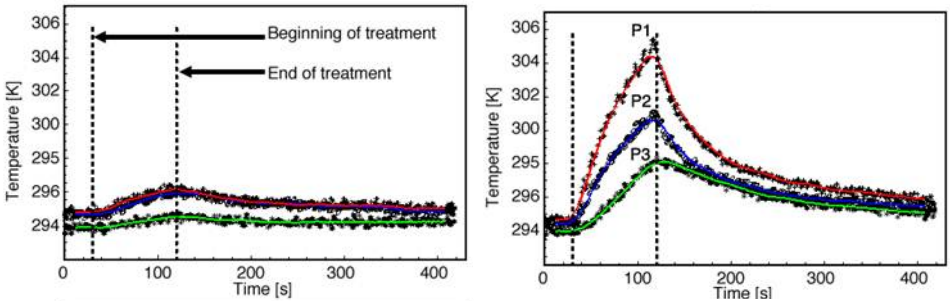

Figure 2: Temperature distribution in (left) 1000 V/cm (voltage-to-distance ratio) and (right) 2000 V/cm IRE protocols. The probes are located at a depth of 1.5 cm at known distances 2.5 mm (P1), 5 mm (P2) and -2.5 mm (P3) from the IRE electrode.

Although the maximum temperature ranges induced on the brain serve as a relative indicator of effects, it is desirable to calculate the percentage of thermal damage at each of these points from the various processes described in [14, 16]. These are tabulated in

Table **3**, where it can be seen that the maximum probability of combined thermal damage is 0.649%, and occurs for the 2000 V/cm protocol at probe 1.

Table 3: Thermal damage probability (%) for each location from the *ex-vivo* IRE protocol.

DAMAGE PROCESS	LOCATION	1000 V/CM	2000 V/CM
Microvascular Blood Flow Stasis	P1	3.420E-04	4.788E-02
	P2	3.116E-04	3.466E-03
	P3	1.240E-04	8.820E-04
Cell Death	P1	1.751E-02	5.278E-01
	P2	1.632E-02	8.468E-02
	P3	8.171E-03	3.361E-02
Protein Coagulation	P1	1.888E-02	7.324E-02
	P2	1.823E-02	3.601E-02
	P3	1.289E-02	2.488E-02

5. Conclusion

IRE therapies have proven to be an effective and beneficial focal ablation technique for the treatment of pathologic tissues such as tumors. To the best of our knowledge, all previous studies into the thermal effects of such treatments have been limited to numerical simulations. This study presents the first experiments to measure the temperature in tissue undergoing a typical IRE treatment protocol. It was found that the maximum temperature change in the tissue was 11.2˚C at the closest probe to the electrode, between the two electrodes. An analysis of thermal damage processes showed that, at this point, there was a combined thermal damage probability of only 0.649%, suggesting that even at the site of the greatest observed temperature changes, the thermal effects are negligible. Therefore, it may be concluded that IRE therapies are a result of non-thermal mechanisms to induce cell death.

6. Acknowledgments

This work was supported by the Coulter Foundation. The authors thank Dr. Bonnie Brenseke for help with the experimental protocol.

7. References

1. Davalos, R.V., L.M. Mir, and B. Rubinsky, *Tissue ablation with irreversible electroporation.* Ann Biomed Eng, 2005. **33**(2): p. 223-31.
2. Weaver, J.C. and Y.A. Chizmadzhev, *Theory of electroporation: A review.* Bioelectrochem Bioenerg, 1996. **41**: p. 135-60.
3. Rubinsky, B., ed. *Irreversible Electroporation*. 2010, Springer Berlin Heidelberg.
4. Lee, E.W., C.T. Loh, and S.T. Kee, *Imaging guided percutaneous irreversible electroporation: ultrasound and immunohistological correlation.* Technol Cancer Res Treat, 2007. **6**(4): p. 287-94.
5. Lee, R.C. and F. Despa. *Distinguishing Electroporation from Thermal Injuries in Electrical Shock by MR Imaging*. in *Engineering in Medicine and Biology 27th Annual Conference*. 2005. Shanghai, China: IEEE.
6. Garcia, P.A., J.H. Rossmeisl, J. Robertson, T.L. Ellis, and R.V. Davalos, *Pilot study of irreversible electroporation for intracranial surgery.* Conf Proc IEEE Eng Med Biol Soc, 2009. **1**: p. 6513-6.
7. Davalos, R.V., D.M. Otten, L.M. Mir, and B. Rubinsky, *Electrical impedance tomography for imaging tissue electroporation.* IEEE Trans. on Biomedical Engineering, 2004. **51**(5): p. 761-767.
8. Davalos, R.V., D.M. Otten, and B. Rubinsky, *A feasibility study for electrical impedance tomography as a means to monitor tissue electroporation for molecular medicine.* IEEE Trans. on Biomedical Engineering, 2002. **49**(4): p. 400-403.
9. Neal II, R.E., R. Singh, H.C. Hatcher, N.D. Kock, S.V. Torti, and R.V. Davalos, *Treatment of breast cancer through the application of irreversible electroporation using a novel minimally invasive single needle electrode.* Breast Cancer Research and Treatment, 2010.
10. Onik, G., P. Mikus, and B. Rubinsky, *Irreversible Electroporation: Implications for Prostate Ablation.* Technol Cancer Res Treat, 2007. **6**(4): p. 295-300.
11. Maor, E., A. Ivorra, J. Leor, and B. Rubinsky, *The Effect of Irreversible Electroporation on Blood Vessels.* Technol Cancer Res Treat, 2007. **6**(4): p. 307-312.
12. Rubinsky, B., G. Onik, and P. Mikus, *Irreversible Electroporation: A New Ablation Modality - Clinical Implications.* Technol Cancer Res Treat, 2007. **6**(1): p. 37-48.
13. Davalos, R.V., B. Rubinsky, and L.M. Mir, *Theoretical analysis of the thermal effects during in vivo tissue electroporation.* Bioelectrochemistry, 2003. **61**(1-2): p. 99-107.
14. Sherar, M.D., J.A. Moriarty, M.C. Kolios, J.C. Chen, R.D. Peters, L.C. Ang, R.S. Hinks, R.M. Henkelman, M.J. Bronskill, and W. Kucharcyk, *Comparison of thermal damage calculated using magnetic resonance thermometry, with magnetic resonance imaging post-treatment and histology, after interstitial microwave thermal therapy of rabbit brain.* Phys Med Biol, 2000. **45**(12): p. 3563-76.
15. Tropea, B.I. and R.C. Lee, *Thermal injury kinetics in electrical trauma.* J Biomech Eng, 1992. **114**(2): p. 241-50.
16. Lee, R.C., D. Zhang, and J. Hannig, *Biophysical injury mechanisms in electrical shock trauma.* Annual Review of Biomedical Engineering, 2000. **2**(1): p. 477-509.
17. Davalos, R.V. and B. Rubinsky, *Temperature considerations during irreversible electroporation.* International Journal of Heat and Mass Transfer, 2008. **51**(23-24): p. 5617-5622.
18. Brown, S.L., J.W. Hunt, and R.P. Hill, *Differential thermal sensitivity of tumor and normal tissue microvascular response during hyperthermia.* International Journal of Hyperthermia, 1992. **8**(4): p. 501-514.
19. Borrelli, M.J., L.L. Thompson, C.A. Cain, and W.C. Dewey, *Time-temperature analysis of cell killing of BHK cells heated at temperatures in the range of 43.5 degrees C to 57.0 degrees C.* International Journal of Radiation Oncology Biology Physics, 1990. **19**(2): p. 389-399.
20. Jacques S.L., Newman C,, and He X Y, *Thermal coagulation of tissues: liver studies indicate a distribution of rate parameters, not a single rate parameter, describes the coagulation process* in *Advances in Biological Heat and Mass Transfer* 1991, J McGrath: New York: ASME. p. 71-73.